ACETOHYDROXAMATOIRON (III) COMPLEXES: THERMODYNAMICS OF FORMATION AND TEMPERATURE DEPENDENT SPECIATION

Fabrice P. L. Andrieux*[†], Colin Boxall[†], Robin J. Taylor[‡]

[†] John Tyndall Institute for Nuclear Research, University of Central Lancashire, Preston, PR1 2HE, UK

[‡]Nexia Solutions Ltd, British Technology Centre, Sellafield, Seascale, Cumbria CA20 1PG, UK

* To whom all correspondence should be addressed. John Tyndall Institute for Nuclear Research, University of Central Lancashire, Preston, PR1 2HE, UK. Tel.: +44 1772 893578; fax: +44 1772 892996; e-mail: fandrieux@uclan.ac.uk

Abstract

Studies of the thermodynamics of formation of the acetohydroxamatoiron(III) complexes were carried out in acidic media at temperatures ranging from 293 to 323 K. Through the isolation of the unique UV –visible spectra of all three complexes, it was possible to determine their formation constants and deduce enthalpies and entropies of formation as well as their molar absorptivities. The enthalpies of formation of the mono-, bis- and trisacetohydroxamatoiron(III) complexes were found to be –56.4, –17.09 and +19.74 $kJ \bullet mol^{-1}$, respectively. Following the determination of the enthalpy and entropy of formation of these complexes, speciation diagrams were calculated for the complexes at temperatures ranging from 293 to 323 K.

Keywords:

Acetohydroxamic acid, ferric ions, complexation, speciation, thermodynamic constants, molar absorptivity

1. Introduction

Simple hydroxamic acids (XHA) are hydrophilic organic compounds with the general formula RCONHOH and so can act as O,O donor ligands with high affinities for hard cations such as Fe^{3+}, Np^{4+} and Pu^{4+} with which they form 5 membered chelate rings [1-3].

They have a wide range of applications in many fields, including as enzyme inhibitors, soil enhancers, fungicides, mutagens, carcinogens, DNA cleavers, drug delivery systems [4], ion exchange [5] and materials research [4]. Siderophores such as the desferrioxamines contain multiple hydroxamate functionalities and are naturally occurring ligands specifically used by fungi for the sequestration of iron from the environment [6-8]. The potential role of such hydroxamate siderophores in the mobilisation of actinide ions within the environment has also been considered [9]. More recently, XHAs have also been identified as useful reagents for the control of Pu and Np in advanced Purex and UREX processes proposed for the processing of spent nuclear fuel [10]. In such separation processes, U, Np and Pu are separated according to oxidation state specific aqueous/non aqueous solvent extraction in the presence of aceto-hydroxamic acid [3].

It is also well known that hydroxamic acids are susceptible to hydrolysis, particularly in acidic solutions [4]. Whilst there have been many studies of hydroxamic acid hydrolysis and their complexation reactions with Fe(III) ions, there have been relatively few studies of the stability of the Fe(III)-hydroxamate complexes towards hydrolysis. We have previously reported on the kinetics of the hydrolysis of hydroxamic acids both in free solution and when bound to metal ions and developed a kinetic model describing this process at ambient temperatures [11,13]. However, the

applications of hydroxamic acids in biological-related fields requires an understanding of the behaviour of these systems at temperature of biological interest, for example *in vivo* (310K) or temperatures at which proteins start to denature (~ 325K) [14]. Additionally, the temperature dependencies of the equilibrium constants are useful in gaining a better understanding of the complexation processes and the role of enthalpy and entropy in complex formation. As a precursor to any temperature-dependent study of Fe(III)-AHA hydrolysis, comprehensive and reliable thermodynamic data are required on the Fe(III)-AHA complexation reactions, which is the focus of this report.

Furthermore, we are applying the kinetic models developed for the Fe(III)-AHA system to the kinetics of the hydrolysis of hydroxamic acids when bound to actinide ions such as Pu^{4+} and Np^{4+} in support of advanced Purex and UREX processes [12]. In this context, Fe(III) is a useful non-radioactive analogue for interrogating the complexation behaviour of actinides.

Thus, a study of the temperature dependence of the speciation of the Fe^{3+}–AHA system will both provide a useful addition to the thermodynamic database of Fe(III) in its own right and support advanced Purex/UREX process development through its role as a non-active analogue of e.g. the Np^{4+}–AHA system.

As mentioned previously, hydroxamic acids readily form stable complexes with Fe^{3+} ions according to reactions described in eqs. 1-3:

$$Fe^{3+} + HL \overset{K_1}{\rightleftharpoons} FeL^{2+} + H^+ \qquad K_1 = \frac{[FeL^{2+}][H^+]}{[Fe^{3+}][HL]} \qquad (1)$$

$$FeL^{2+} + HL \overset{K_2}{\rightleftharpoons} FeL_2^{+} + H^+ \qquad K_2 = \frac{[FeL_2^{+}][H^+]}{[FeL^{2+}][HL]} \qquad (2)$$

$$FeL_2^+ + HL \xrightleftharpoons{K_3} FeL_3 + H^+ \qquad K_3 = \frac{[FeL_3][H^+]}{[FeL_2^+][HL]} \qquad (3)$$

where L represents the deprotonated acetohydroxamato ligand and all equilibrium constants are calculated from concentrations rather than activities.

Values of the equilibrium constant for the formation of the monoacetohydroxamatoiron(III) complex were reported in the literature with Monzyk *et al.* [8] suggesting $K_1 = 109$ without specifying an equilibrium temperature, while Schwarzenbach *et al.* [15] report a value for the $\log K_1 = 2.28$ at 293 K, corresponding to $K_1 = 190.5$. The inconsistency of these values together with a lack of data pertaining to their temperature dependence has prompted us to conduct our own determination of values for K_1, K_2 and K_3. This, we have done through measurement of the electronic absorption spectra (EAS) of a range of mixtures of the three Fe(III)-AHA complexes and the development of a simple analytical method for the extraction of values of equilibrium constants from those spectra. We have also deployed this method for the measurement of the temperature dependence of these equilibrium constants prior to the construction of useful temperature dependent speciation diagrams.

2. Experimental Methods

2.1. Materials

All reagents, including HNO_3 (70%, AnalaR, BDH Chemicals Ltd., Poole, Dorset, UK) and AHA (Sigma-Aldrich Ltd, UK) were obtained from reputable suppliers (Aldrich, Fluka) at the highest available purity and used as received. AHA was stored

in a refrigerator at 4 °C in order to prevent its decomposition. Solutions were prepared using doubly distilled water, produced by a home-made still and further purified by a deionisation system (E pure model 04642, Barnstead / Thermodyne, Dubuque, Iowa, USA) to a resistivity of 1.8 x 10^5 Ω m.

2.2. Experimental limitations derived from Iron(III) hydrolysis.

It is well known that Fe^{3+} readily hydrolyses in water in accordance with:

$$Fe^{3+} + H_2O \rightleftharpoons FeOH^{2+} + H^+ \quad (4)$$

This equilibrium is the first step in a series of deprotonation / polymerisation reactions that ultimately result in the formation of ferric hydroxides and oxyhydroxides. Using the most recently published, critically assessed Gibbs energies of formation of the various species involved [16,17], the equilibrium constant for this first deprotonation can be calculated as being equal to 6.78 x 10^{-3} at 298 K, corresponding to a $pK_a(Fe^{3+})$ of 2.17. Thus, as hydrolysis to form $Fe(OH)^{2+}$ will become significant above pH = 2.17 at 298 K, only those data recorded at pH = 2.1 and below at this temperature will be subjected to rigorous experimental interpretation and analysis.

However, our study extends beyond T = 298 K to determine the temperature dependence of K_1-K_3 in the temperature range 293-323 K. The equilibrium constant for the reaction shown in eq. 4 has been studied as a function of temperature (T = 298-353 K) and ionic strength (I = 0.1-2.67 M) in perchlorate media by Sapieszko *et al.* [18] Using their data, we have calculated that, in order to prevent significant formation of hydrolysed iron (III) under the conditions of our experiments (T = 293-323 K, and I ~ 0.1M), the value of the pH to be used in the determination of the equilibrium constants of formation of the acetohydroxamatoiron (III) complexes

should not exceed 1 at T > 300 K. Any data presented at pH > 1 at T > 300 K is shown for the purposes of context only.

2.3. Procedures

UV-visible absorbance spectra of complex and complex precursor solutions were measured by spectrophotometry (Diode Array model 8452A, Hewlett Packard, USA) fitted with a HP89090A Peltier temperature controller. Solutions for spectroscopic measurement were prepared from stock (Fe(III)) or freshly made solutions (AHA, prepared immediately prior to experiment) and pipetted into an optical cuvette (pathlength 1 cm). The complexant (AHA) was added last. The volume of complexant required was always small and had no effect on the temperature of the receiving solution when added. The spectra were then measured as soon as possible after mixing. All experiments were performed at pH (= $-\log_{10}[H^+]$) < 1 in order to minimise hydrolysis of free ferric ions and the formation of iron hydroxides and oxyhydroxides.

3. Results and Discussions

Prior to reporting our EAS measurements, we shall first describe briefly our simple approach for the extraction of equilibrium constants from those spectra.

In a solution containing any amounts of iron and acetohydroxamic acid, the concentrations of the various species in solution obtained as a result of the establishment of equilibria described in eqs. 1-3 may be expressed as follows:

$$[Fe^{3+}] = [Fe^{3+}]_i - \xi_1 - \xi_2 - \xi_3 \qquad (5)$$

$$[HL] = [HL]_i - \xi_1 - 2\xi_2 - 3\xi_3 \quad (6)$$

$$[FeL^{2+}] = \xi_1 \quad (7)$$

$$[FeL_2^{+}] = \xi_2 \quad (8)$$

$$[FeL_3] = \xi_3 \quad (9)$$

$$[H^+] = [H^+]_i + \xi_1 + 2\xi_2 + 3\xi_3 \quad (10)$$

where $[Fe^{3+}]_i$, $[HL]_i$ and $[H^+]_i$ represent the initial concentrations of iron(III), acetohydroxamic acid and nitric acid, respectively.

3.1. Determination of K_1 and the molar absorptivity of FeL^{2+}

Eq. 11 shows K_1 expressed in terms of the parameters defined in eqs. 5-10 under conditions where $\xi_2 \approx 0$ and $\xi_3 \approx 0$ i.e. in the effective absence of the 2:1 or higher Fe(III)-AHA complexes

$$K_1 = \frac{\xi_1 \times \left([H^+]_i + \xi_1\right)}{\left([Fe^{3+}]_i - \xi_1\right) \times \left([HL]_i - \xi_1\right)} \quad (11)$$

At any given temperature, eq. 11 contains two unknown parameters: K_1 which is constant and ξ_1, dependent on the concentrations of the other components of the system. Thus, eq. 11 may only be solved if two datasets are recorded under different experimental conditions (e.g. at different pH). The ratio of the absorbances, Abs, for these two experiments being equivalent to the ratio of the mono-complex concentrations, provided the absorbance of the complex is measured at a wavelength that is non-coincident with the absorbance envelope of all other components in solution (H^+, HL, Fe^{3+}). Preliminary spectral measurements (not shown) indicate that this condition is satisfied in the wavelength range 800 to 350 nm. Accordingly,

absorbances were measured at λ = 510 nm and eq. 11 may be rewritten for the two arbitrarily numbered experiments as a function of only one unknown parameter (ξ_1):

$$K_1 = \frac{\xi_{1,1}\left([H^+]_{i,1} + \xi_{1,1}\right)}{\left([Fe^{3+}]_{i,1} - \xi_1\right)\left([HL]_{i,1} - \xi_{1,1}\right)} = \frac{x\xi_{1,1}\left([H^+]_{i,2} + x\xi_{1,1}\right)}{\left([Fe^{3+}]_{i,2} - x\xi_{1,1}\right)\left([HL]_{i,2} - x\xi_{1,1}\right)} \qquad (12)$$

with $$x = \frac{\left[FeL^{2+}\right]_2}{\left[FeL^{2+}\right]_1} = \frac{\xi_{1,2}}{\xi_{1,1}} = \frac{Abs_2}{Abs_1}$$

where the additional subscript refers to the arbitrarily attributed experiment number.

Eq. 12 may be rearranged into the quadratic eq. 13 which is soluble provided that both experiments are recorded with known total concentrations of H^+, HL and Fe^{3+}. The resulting roots can then be inspected and the one corresponding to a positive value of the complex concentration lower than the total amount of acetohydroxamic acid, selected as $\xi_{1,1}$.

$$\begin{aligned}&\left(x^2\left([HL]_{i,1} + [Fe^{3+}]_{i,1} + [H^+]_{i,1}\right) - x\left([HL]_{i,2} + [Fe^{3+}]_{i,2} + [H^+]_{i,2}\right)\right){\xi_{1,1}}^2 + \\ &\quad\left(-x^2[Fe^{3+}]_{i,1}[HL]_{i,1} + x\left[[H^+]_{i,2}\left([HL]_{i,1} + [Fe^{3+}]_{i,1}\right) - \right.\right. \\ &\qquad\left.\left.[H^+]_{i,1}\left([HL]_{i,2} + [Fe^{3+}]_{i,2}\right)\right] + [Fe^{3+}]_{i,2}[HL]_{i,2}\right)\xi_{1,1} + \\ &\qquad\left([H^+]_{i,1}[Fe^{3+}]_{i,2}[HL]_{i,2} - x[H^+]_{i,2}[Fe^{3+}]_{i,1}[HL]_{i,1}\right) = 0\end{aligned} \qquad (13)$$

As implied above, for K_1 to be determined from this treatment, the spectrum of the mono-complex must be measured in the absence of bis- or tris- complexes in solution. Preliminary speciation calculations [11] suggest that this may be achieved by recording the spectra in a large excess of iron (III). Thus, three solutions were prepared containing 50 mol•m^{-3} Fe^{3+} and 1 mol•m^{-3} AHA at pH = 0.2, 0.71 and 0.85,

respectively. Fig.1 shows a typical spectrum recorded from the solution at pH = 0.2 at T = 313K. Values of $\xi_{1,1}$ were then calculated for each of the three pairs of solution, and an average K_1 determined. This procedure was repeated at 293, 298, 303, 313, and 323 K to obtain the equilibrium constant as a function of temperature. Values of K_1 as a function of temperature are given in table 1.

If it is assumed that ΔH^o and ΔS^o are invariant with temperature, the Van't Hoff isochore may be written as:

$$\ln K_1 = -\frac{\Delta H^o}{RT} + \frac{\Delta S^o}{R} \qquad (14)$$

In accordance with eq. 14, Fig. 2 shows a plot of ln K_1 vs. T^{-1} for the data of table 1. The linearity of this plot justifies our assumption of T-invariant ΔH^o and ΔS^o in the derivation of eq. 14, use of which allows calculation of their values as –56.4 kJ•mol^{-1} and –158.2 J•mol^{-1}•K^{-1}, respectively. These values indicate that the formation of the mono- complex is accompanied by a loss of entropy and so is enthalpically driven.

Using the spectra obtained above, together with the concentrations of the mono-complex calculated in the computation of K_1, it is possible to obtain the value of the molar absorptivity (ε in m^2•mol^{-1}) for this complex, *via* Beer's law:

$$\text{Abs} = \varepsilon\, l\, \xi_1 \qquad (15)$$

where l is the width of the cuvette in m, and ξ_1 is expressed in mol•m^{-3}. The molar absorptivity for the monoacetohydroxamatoiron (III) complex was found to be ε_1 = 101 ± 1 m^2•mol^{-1}.

3.2. Determination of K_2 and the molar absorptivity of FeL_2^+

Determination of K_2 necessitates study of solutions wherein the mono- and bis-complexes dominate and the tris- complex is absent. Farkas *et al.* [19] suggest that the transition of the dominant species from mono- to bis- to tris- as ligand concentration is increased can be followed by the absorption maximum moving from 510 to 470 to 420 nm for the mono-, bis- and tris- complexes, respectively. Consequently solution conditions that give rise to λ_{max} between 510 and 470 nm might be expected to give rise to a system wherein the concentration of the tris- complex can be considered to be approximately zero, especially if λ_{max} is closer to 510 than 470 nm. In the pH range 0.2 – 0.9, this condition was found to be satisfied experimentally for $[Fe^{3+}]$ and [HL] values of 0.5 mol•m^{-3} and 200 mol•m^{-3}, respectively. The assumption that the concentration of the tris- complex can be neglected at these $[Fe^{3+}]$ and [HL] values over this pH range is supported by preliminary results in our previous paper [11].

In order to determine values of K_2 from solutions containing a mixture of the mono- and bis-acetohydroxamato complexes, the contributions of each species to the observed spectra must first be deconvoluted. Spectra of the mono-complex alone were obtained in the determination of K_1. These may be normalised at λ_{max} = 510 nm and averaged over the wavelength range considered here (350-800 nm) and used to partition the signal obtained from a mixture of both complexes according to its source (mono- or bis- complex). In this process the normalised peak obtained for the mono-complex is multiplied by a scaling factor and subtracted from the real solution spectra, revealing the spectra of the bis- complex. Increasing the value of the scaling factor displaces the peak calculated for the bis- complex toward lower wavelengths. The fit is complete when the λ_{max} of the absorbance attributed to the bis-complex spectrum reaches λ_{max} reported for this complex in the literature (λ_{max} = 470 nm) [2]. This procedure is repeated for each pH (0.4, 0.6 and 0.74) at all temperatures studied (T =

293-323 K). All three spectra obtained at pH 0.61 and T = 323 K – separate mono-, separate bis- and mono- and bis- together – are overlaid in Fig.3.

From this series of deconvoluted spectra, it is possible to determine the concentration of the mono-complex (from the molar absorptivity calculated in section 3.1 and the deconvoluted absorbance at 510nm) and the absorbance at λ_{max} = 470 nm due to the presence of the bis- complex. Using an argument similar to that advanced to determine K_1, it is then possible to calculate the concentration of the bis- complex and the value of K_2.

Stepwise or overall equilibrium constants may be reported for the formation of the Fe(III)-AHA complexes. Although the mathematical treatment associated with the calculation of the concentration of the bis- complex with the former may be simpler, the latter explicitly takes the formation of the mono- complex into account. We therefore devise a solution using the overall equilibrium constant for FeL_2^+ formation, β_2, assuming the simultaneous formation of the mono- and bis- complexes. β_2 (= K_1 K_2) is given by:

$$\beta_2 = \frac{[FeL_2^+][H^+]^2}{[Fe^{3+}][HL]^2} \tag{16}$$

which, assuming that $\xi_3 \approx 0$, may be expressed as a function of the equilibrium concentrations given in eqs. 5-10, as:

$$\beta_2 = \frac{\xi_2\left([H^+]_i + \xi_1 + 2\xi_2\right)^2}{\left([Fe^{3+}]_i - \xi_1 - \xi_2\right)\left([HL]_i - \xi_1 - 2\xi_2\right)^2} \tag{17}$$

Eq. 17 contains two unknowns β_2 and ξ_2; thus, two data sets are again required for their evaluation. It is possible to calculate the value of ξ_2, by measuring the absorbance of two samples at different pH values but the same temperature at λ_{max} = 470 nm and dividing one absorbance value by the other. This results in a soluble system of two equations with two unknowns given in eq. 18:

$$\beta_2 = \frac{\xi_{2,1}\left([H^+]_{i,1} + \xi_{1,1} + 2\xi_{2,1}\right)^2}{\left([Fe^{3+}]_{i,1} - \xi_{1,1} - \xi_{2,1}\right)\left([HL]_{i,1} - \xi_{1,1} - 2\xi_{2,1}\right)^2} = \frac{y\xi_{2,1}\left([H^+]_{i,2} + \xi_{1,2} + 2y\xi_{2,1}\right)^2}{\left([Fe^{3+}]_{i,2} - \xi_{1,2} - y\xi_{2,1}\right)\left([HL]_{i,2} - \xi_{1,2} - 2y\xi_{2,1}\right)^2} \quad (18)$$

with $$y = \frac{[FeL_2^+]_2}{[FeL_2^+]_1} = \frac{\xi_{2,2}}{\xi_{2,1}} = \frac{Abs_2}{Abs_1}$$

where the additional subscripts again refer to the arbitrarily attributed experiment number. Rearranging eq. 18 yields eq. 19; this is 6th order with regards to the unknown $\xi_{2,1}$ and may not be trivially solved analytically but may be solved by a straightforward computation.

$$\xi_{2,1}\left([H^+]_{i,1} + \xi_{1,1} + 2\xi_{2,1}\right)^2\left([Fe^{3+}]_{i,2} - \xi_{1,2} - y\xi_{2,1}\right)\left([HL]_{i,2} - \xi_{1,2} - 2y\xi_{2,1}\right)^2 - y\xi_{2,1}\left([H^+]_{i,2} + \xi_{1,2} + 2x\xi_{2,1}\right)^2\left([Fe^{3+}]_{i,1} - \xi_{1,1} - \xi_{2,1}\right)\left([HL]_{i,1} - \xi_{1,1} - 2\xi_{2,1}\right)^2 = 0 \quad (19)$$

A spreadsheet is generated calculating the values of the left hand side of eq. 19 as a function of $\xi_{2,1}$. The values of ξ_1 are calculated using the absorbance measured from the deconvoluted spectra and the molar absorptivity measured in section 3.1. The roots of eq. 19 are then inspected and the single root that corresponds to a physically

and mathematically possible bis- complex concentration (i.e. $0 < \xi_{2,1} \leq [Fe^{3+}]_i$) is selected.

Substitution of this value of $\xi_{2,1}$ into eq. 2 then enables the calculation of K_2. With three datasets available for each temperature considered, three values of K_2 may be calculated and an average taken. Table 2 presents the calculated values of K_2 for each temperature. The value of 2.56 calculated at 298K is in fair agreement with the literature value of 2.04 provided by Arif-Kazmi *et al*. [20].

Fig.4 shows the K_2 data of table 2 plotted in accordance with the K_2 analogue of eq. 14 and in analogy to Fig.2 and again assuming that the standard enthalpy and entropy of reaction for the formation of the bis-complex are invariant with temperature over the range studied. The linearity of the plot of Fig.4 supports this assumption and, in conjunction with eq. 14, allows for the determination of values of ΔH^o and ΔS^o for the formation of the bis- complex of –17.09 kJ•mol^{-1} and –49.7 J•mol^{-1}•K^{-1}, respectively. As for the mono- complex, both ΔH^o and ΔS^o for the formation of the bis- complex are negative, indicating that the process is accompanied by a loss of entropy and so is enthalpically driven.

Using the deconvoluted spectra obtained earlier in this section, together with the concentrations of the bis- complex calculated in the computation of K_2, it is possible to obtain the value of the molar absorptivity for this complex, *via* Beer's law (eq. 15), which is found to be $\varepsilon_2 = 165 \pm 14$ m^2•mol^{-1}.

3.3. Determination of K_3. and the molar molar absorptivity of FeL_3

Using analoguous arguments as those advanced in section 3.2 for the determination of K_2 it is possible to identify preliminary solution conditions under which only the bis-

and tris- complexes are present. Again, preliminary calculations [11] indicate that, in the pH range 0.2–0.9, this condition is satisfied for $[Fe^{3+}]_i$ and $[HL]_i$ values of 0.4 mol•m^{-3} and 6300 mol•m^{-3}, respectively.

The signals from each compound in each solution studied were deconvoluted by following the methodology described in section 3.2 i.e. by subtracting the normalised averaged spectra of the bis- complex from the real solution spectrum in order to isolate that of the tris- complex. Again, the literature value of the wavelength of maximum absorption for the tris- complex (λ_{max} = 420 nm) [7] was used to determine the value of the scaling factor.

Evaluation of the overall equilibrium constant for the formation of the tris-complex β_3 is again preferred over the stepwise equilibrium constant K_3 as it explicitly takes the presence of mono- and bis- complexes into account. β_3 (= K_3 K_2 K_1) is given by:

$$\beta_3 = \frac{[FeL_3][H^+]^3}{[Fe^{3+}][HL]^3} \tag{20}$$

which may be expressed as a function of the equilibrium concentrations given in eqs. 5-10, assuming that the entirety of iron is complexed to form the bis- and tris- complexes and that no mono- complex is present ($\xi_1 \approx 0$). This gives:

$$\beta_3 = \frac{\xi_3\left([H^+]_i + 2\xi_2 + 3\xi_3\right)^3}{\left([Fe^{3+}]_i - \xi_2 - \xi_3\right)\left([HL]_i - 2\xi_2 - 3\xi_3\right)^3} \tag{21}$$

Eq. 21 contains two unknowns, β_3 and ξ_3. Thus, as in the analysis of eqs. 11 and 17, two data sets are required. Measurement of the absorbance of the tris- complex at λ_{max} = 420 nm at two different pH values, allows us to write:

$$\beta_3 = \frac{\xi_{3,1}\left([H^+]_{i,1} + 2\xi_{2,1} + 3\xi_{3,1}\right)^3}{\left([Fe^{3+}]_{i,1} - \xi_{2,1} - \xi_{3,1}\right)\left([HL]_{i,1} - 2\xi_{2,1} - 3\xi_{3,1}\right)^3} = \frac{z\xi_{3,1}\left([H^+]_{i,2} + 2\xi_{2,2} + 3z\xi_{3,1}\right)^3}{\left([Fe^{3+}]_{i,2} - \xi_{2,2} - z\xi_{3,1}\right)\left([HL]_{i,2} - 2\xi_{2,2} - 3z\xi_{3,1}\right)^3} \quad (22)$$

with $z = \frac{[FeL_3]_2}{[FeL_3]_1} = \frac{\xi_{3,2}}{\xi_{3,1}} = \frac{Abs_2}{Abs_1}$

where the additional subscripts are again the arbitrarily assigned experiment number. Rearranging eq. 22 yields eq. 23 which is 8th order with regards to the unknown $\xi_{3,1}$ and may again be solved by computation, in analogy to eq. 19.

$$z\xi_{3,1}\left([H^+]_{i,2} + 2\xi_{2,2} + 3z\xi_{3,1}\right)^3\left([Fe^{3+}]_{i,1} - \xi_{2,1} - \xi_{3,1}\right)\left([HL]_{i,1} - 2\xi_{2,1} - 3\xi_{3,1}\right)^3 - \xi_{3,1}\left([H^+]_{i,1} + 2\xi_{2,1} + 3\xi_{3,1}\right)^3\left([Fe^{3+}]_{i,2} - \xi_{2,2} - z\xi_{3,1}\right)\left([HL]_{i,2} - 2\xi_{2,2} - 3z\xi_{3,1}\right)^3 = 0 \quad (23)$$

The roots are then inspected and the single root that corresponds to a physically and mathematically possible value of the tris- complex concentration (i.e. $0 < \xi_{3,1} \leq [Fe^{3+}]_i$) is selected. Substitution into eq. 3 then allows calculation of K_3. Table 3 presents the values of K_3 calculated from the three datasets available for each temperature. The value measured at 298K (17.9×10^{-3}) is of the same order as the literature value of 7.4×10^{-3} provided by Arif-Kazmi *et al*. [20].

Fig.6 shows the data of table 3 plotted in an analogous fashion as the data of tables 1 and 2 are plotted in Figs.2 and 4, again assuming that ΔH^o and ΔS^o for the formation of the tris- complex are invariant with temperature over the range studied. Again, the linearity of the plot in Fig.6 supports this assumption. From Fig.6, and the K_3 analogue of eq. 14, ΔH^o and ΔS^o are found to be +19.74 kJ•mol^{-1} and +32.93 J•mol^{-1}•K^{-1} respectively. In contrast to the formation of the mono- and bis- complexes, ΔS^o

and ΔH^o for the formation of the tris- complex are both positive, indicating that the process is entropically driven.

Using the deconvoluted spectra obtained earlier in this section, together with the concentrations of the tris- complex calculated in the computation of K_3, it is possible to obtain the value of the molar absorptivity for this complex, *via* Beer's law, eq. 15, which is found to be $\varepsilon_3 = 363 \pm 29$ $m^2 \bullet mol^{-1}$.

3.4. Speciation of the Fe-AHA complexes

With values of K_1, K_2 and K_3 as a function of temperature now computed, it is possible to generate speciation diagrams for the Fe(III)-AHA system taking into account pH, pHL ($= -\log_{10}[HL]$) and temperature.

Fig.7 shows the speciation diagram calculated as a function of acetohydroxamic acid concentration (given as pHL) for a range of nitric acid concentrations at a temperature of 293 K. For a given pHL value, an increase in pH results in an increase in the order of the complex formed from free metal ion to mono-, bis- and tris- complex.

Fig.8 shows the speciation diagram calculated as a function of pH for a range of acetohydroxamic acid concentrations at a temperature of 293 K. As expected from eqs. 1-3, an increase in the concentration of AHA (decrease in pHL) results in the formation of higher order acetohydroxamatoiron(III) complexes.

Fig.9 shows the speciation diagram calculated as a function of pHL for a nitric acid concentration of 100 $mol \bullet m^{-3}$ at a range of temperatures. Fig.10 shows the speciation diagrams calculated as a function of pH for a total acetohydroxamic acid concentration of 250 $mol \bullet m^{-3}$, again at a range of temperatures.

From both Figs.9 and 10 it can be seen that increasing temperature is detrimental to the formation of the mono- and bis- complexes, which is to be expected from the exothermic character of these reactions. However the formation of the unbound metal (especially at low pH) and the tris- complex (especially at high pH) are favoured by rising T, due to the displacement of the equilibria forming the bis- and mono- complexes as well as the endothermic character of the reaction described by eq. 3.

3.5. Verification of the assumptions made in the determination of K_1, K_2 and K_3.

The calculations of K_1, K_2, and K_3 functions of temperature were each conducted under conditions where it was assumed that one or more of the acetohydroxamatoiron(III) complexes were present in negligible amounts only. These assumptions may now be verified by building speciation diagrams for the pH range and specific concentrations of AHA and Fe(III) used in the each of these experiments.

Fig.11 shows the speciation diagrams calculated for the conditions under which K_1 was determined ($[Fe^{3+}]$ = 50 mol•m^{-3}, [AHA] = 1 mol•m^{-3}) at 293 and 323 K. Over the pH range considered for this study (pH = 0.2 – 0.85), a maximum of 0.30% of all complexed iron is present as either the bis- or the tris- complex, which supports the assumption made in section 3.1 that the mono- complex and free iron are the predominant species in solution.

Fig.12 shows the speciation diagrams calculated for the conditions under which K_2 was determined ($[Fe^{3+}]$ = 0.5 mol•m^{-3}, [AHA] = 200 mol•m^{-3}) at 293 and 323K. Over the pH range studied (pH = 0.4 – 0.74), a maximum of 2.67% of all complexed Fe(III) is present as the trisacetohydroxamatoiron species, the remainder being present as either the mono- or bis- complex, thus validating our assumption in section 3.2 that

the mono- and bis- complexes are the predominant acetohydroxamatoiron species in solution.

Fig.13 shows the speciation diagrams calculated for the conditions under which K_3 was determined ($[Fe^{3+}]$ = 0.4 mol•m^{-3}, [AHA] = 6300 mol•m^{-3}) at 293 and 323K. Over the range of pH considered for this study (pH = 0.4 – 0.93), a maximum of 2.69% of the complexed iron is available as the mono- complex, the rest being present as either the bis- or tris- complex. Again, this supports our assumption in section 3.3 that the mono- complex is present in negligible amounts compared to the higher complexes, so allowing us to ignore it in determination of K_3.

The above determined limits on the assumptions underpinning the spectral deconvolution technique, as well as the molar absorptivities for each complex (summarised in table 4) now allow us to advance an explanation for the comparatively large standard deviation values observed with respect to the value of K_2.

These may arise from the combined effect of the relatively low concentrations of the various interferents and their respective molar absorptivities. For example, the interferent in the case of the determination of K_2 is the tris- complex, which has a molar absorptivity value 2.2x higher than that of the bis- complex and 3.6x that of the mono-complex, amplifying its influence on the measured absorbance. Conversely, the determination of K_3 neglects the presence of the mono-complex (actually present in levels similar to the levels of the tris- complex in the determination of K_2), which has a molar absorbtivity 0.6x that of the bis- complex and 0.28x that of the tris- complex. As an impurity, it therefore has a proportionately smaller effect on the absorbance-derived determination of K_3 than the tris- complex has on the determination of K_2, and results in a narrower distribution of K_3 values. It should also be noted that the levels

of the bis- and tris- complex in the determination of K_1 are very low (0.3% overall) and thus do not contribute significantly to elevating the standard deviation in the value of K_1 in spite of their greater molar absorptivities.

4. Conclusions

The thermodynamic constants for all three equilibria that obtain in the iron(III)-AHA system have been calculated and the associated enthalpies and entropies for the formation of these complexes have been determined. These are summarised in table 4 together with the molar absorptivity for each of the three complexes. These new values have been used to calculate speciation diagrams for the Fe-AHA system as a function of pH, AHA concentration and temperature.

Inspection of the molar absorptivities measured for all three complexes reveal that it increases as the number of ligands bound to the iron increase. This is presumably in line with the greater availability of ligands to contribute to the ligand-to-metal charge transfer bands that dominate the absorption spectra of the Fe(III)-AHA system..

It is of note that as the number of bound ligands increase, the enthalpy and entropy both become progressively more positive, i.e. complexation becomes enthalpically less favourable but entropically more favourable as the L:M ratio increases.

As regards the entropy changes, this probably reflects the entropy being a balance of two effects as individual reactions progress:

(i) The **entropy increases** as a result of the chelate effect, which is probably strong due to the generation of a 5-membered ring as the two solution phase

reagents come together, releasing two water molecules from the inner solvation shell of Fe(III) and a proton from the AHA. Also, the outer sphere ordering of the solvent around the complex decreases as more ligands are added and the overall electrostatic charge on the complex decreases.

(ii) The **entropy decreases** as a result of a low charge density positive charge on the iron complex being partially converted to high charge density positive charge on the proton, with concomitant ordering of solvent around the proton.

In the formation of the mono- complex, process (ii) is presumably dominant but becomes less so as the ligand number increases due to the decrease in charge of the formed complex and so decrease in its influence on the ordering of the solvent. Thus as the influence of (ii) decreases, the impact of (i) becomes proportionately greater until it dominates and the complexation process exhibits an overall favourable formation entropy with the neutral $Fe(AHA)_3$ complex.

The progression in enthalpy suggests that, as the degree of complexation increases, the energy balance between Fe-O bonds breaking (E_{bb}) and bonds forming (E_{bf}) changes from $|E_{bb}| < |E_{bf}|$ in the $Fe(AHA)^{2+}$ to $|E_{bb}| > |E_{bf}|$ in the $Fe(AHA)_3$ complex, i.e. the replacement of two H_2O molecules by an AHA ligand becomes less favourable. This is presumably related to steric considerations as the hydroxamate ligand is much bulkier than the two water molecules it displaces. Thus, as the number of hydroxamato ligands around the metal increases, the resultant ligand-ligand repulsion forces increase, acting against the enthalpy gained by complexation.

Finally, we have recently developed a speciation dependent kinetic model [11] that allows for the determination of the rate parameter for the hydrolysis of the ligand

within the mono- complex. The speciation diagrams presented in this communication will allow for the desired temperature dependent study of this rate parameter. It will also allow for the extraction of the activiation energy and Arrhenius pre-exponential factor for the process, so providing valuable mechanistic information. This will be the subject of our next paper.

Acknowledgments

The authors thank the Nuclear Decommissioning Authority (NDA) for financial support and for a post-doctoral research fellowship for FA.

References

[1] Muri, E.M.F., Nieto, M.J., Sindelar, R.D., Williamson, J.S.: Hydroxamic Acids as Pharmacological Agents. Current Med. Chem. 9, 1631-1653 (2002)

[2] Desaraju, P., Winston, A.: Synthesis and Iron Complexation Studies of Bis-Hydroxamic Acids. J. Co-ord. Chem. 14, 241-248 (1986).

[3] Carrott, M.J., Fox, O.D., Maher, C.J., Mason, C., Taylor, R.J., Sinkov, S.I., Choppin, G.R.: Solvent Extraction Behaviour of Plutonium (IV) Ions in the Presence of Simple Hydroxamic Acids. Solv. Extr. Ion Exch., 25, 723-746 (2007).

[4] Ghosh, K.K.: Kinetic and Mechanistic Aspects of Acid Catalysed Hydrolysis of Hydroxamic Acids. Indian J. Chem. 36B, 1089-1102 (1997).

[5] Vernon, F.: Chelating Ion Exchangers. The Synthesis and Use of Poly(hydroxamic acid) Resins. Pure and Applied Chem. 54, 2151-2158 (1982)

[6] Raymond, K.N., Freeman, G.E., Kappel, M.J: Actinide-Specific Complexing Agents: Their Structural and Solution Chemistry. Inorg. Chim. Acta. 84, 193-204 (1984)

[7] Renshaw, J.C., Robson, G.D., Trinci, A.P.J., Wiebe, M.G., Livens, F.R., Collinson, D., Taylor, R.J.: Fungal Siderophores: Structures, Functions and Applications. Mycol. Res. 106, 1123-1142 (2002)

[8] Monzyk, B., Crumbliss, A.L.: Mechanism of Ligand Substitution on High-Spin Iron(III) by Hydroxamic Acid Chelators. Thermodynamic and Kinetic Studies on the Formation and Dissociation of a Series of Monohydroxamatoiron (III) Complexes. J. Am. Chem. Soc., 101:21, 6203 (1979).

[9] John, S.G., Ruggiero, C.E., Hersman, L.E., Tung, C.-S., Neu, M.P.: Siderophore Mediated Plutonium Accumulation by Microbacterium Flavescens (JG-9). Environ. Sci. Technol., 35:14, 2942 -2948 (2001).

[10] Birkett, J.E., Carrott, M.J., Fox, O.D., Jones, C.J., Maher, C.J., Roube, C.V., Taylor, R.J., Woodhead, D.A.: Recent Developments in the Purex Process for Nuclear Fuel Reprocessing: Complexant Based Stripping for Uranium - Plutonium Separation. Chimia 59, 898-904 (2005).

[11] Andrieux, F.P.L., Boxall, C., Taylor, R.J.: The Hydrolysis of Hydroxamic Acid Complexants in the Presence of Non-Oxidising Metal Ions 1: Ferric Ions. J. Solution Chem., 36:10, 1201-1217 (2007).

[12] Andrieux, F.P.L., Boxall, C., Mason, C., Taylor, R.J.: The Hydrolysis of Hydroxamic Acid Complexants in the Presence of Non-Oxidising Metal Ions 2: Neptunium (IV) Ions. J. Solution Chem., 37:2, 215-232 (2008).

[13] Carrott, M.J., Fox, O.D., LeGurun, G., Jones, C.J., Mason, C., Taylor, R.J., Andrieux, F.P.L., Boxall, C.: Oxidation-Reduction Reactions of Simple Hydroxamic Acids and Plutonium (IV) Ions in Nitric Acid. Radiochim. Acta, 96:6, 333-344 (2008).

[14] Roos, Y.H.: Phase Transitions and transformations in food systems. In: Handbook of Food Engineering, 2nd edition; Heldmann, D.R., Lund, D.B., Eds., CRC Press, Boca Raton, FL. USA, 328, 2006

[15] Schwarzenbach, G., Schwarzenbach, K.: Hydroxamatkomplexe I. Die Stabilität der Eisen(III)-Komplexe einfacher Hydroxamsäuren und des Ferrioxamins B. Helv. Chim. Acta, 46, 1390-1400 (1963)

[16] Cornell, R.M., Schwertmann, U.: The Iron Oxides, VCH Publishers, New York, Chapter 8, p. 175, 1996.

[17] Heusler, K.E., Lorenz, W.J., Standard Potentials in Aqueous Solution, Bard, A.J., Parsons, R., Jordan, J., Eds., Marcel Dekker Inc., New York, Chapter 14, p.391, 1985.

[18] Sapieszko, R.S., Patel, R.C., Matijevic, E.: Ferric Hydrous Oxide Sols. 2. Thermodynamics of Aqueous Hydroxo and Sulfato Ferric Complexes. J. Phys. Chem. 81, 1061-1068 (1977)

[19] Farkas, E., Kozma, E., Pethő, M., Herlihy, K.M. and Micera, G.: Equilibrium Stidies on copper(II)- and iron(III)- monohydroxamates. Polyhedron. 17, 3331-3342 (1998)

[20] Arif-Kazmi, S., McArdle, J.V.: Kinetics of Formation of Bis- and Tris(acetohydroxamato) Fe(III). J. Inorg. Nucl. Chem. 43, 3031-3034 (1981).

Figure captions

Figure 1: Typical UV-Visible spectra of a solution containing the monoacetohydroxamatoiron(III) complex (Initial solution composition: $[Fe^{3+}]$ = 50 mol•m^{-3} and [AHA] = 1 mol•m^{-3}), recorded at pH = 0.20 at T = 313 K. λ_{max} = 510 nm

Figure 2: ln K_1 vs T^{-1} for the data of table 1, plotted in accordance with eq. 14 and describing the formation of the monoacetohydroxamatoiron(III) complex.

Figure 3: Deconvolution of the spectrum of a solution containing a mixture of mono- (λ_{max} = 510 nm) and bis- (λ_{max} = 470 nm) complexes into separate spectra derived from each species. Initial solution composition: $[Fe^{3+}]$ = 0.5mol•m^{-3} [AHA] 200mol•m^{-3} AHA, recorded at pH 0.61 at T = 323 K

Figure 4: ln K_2 vs. T^{-1} for the data of table 2, plotted in accordance with eq. 14 and describing the formation of the bisacetohydroxamatoiron(III) complex.

Figure 5: Deconvolution of the spectrum of a solution containing a mixture of bis- (λ_{max} = 470 nm) and tris- (λ_{max} = 420 nm) complexes into separate spectra derived from each species. Initial solution composition: $[Fe^{3+}]$ = 0.4 mol•m^{-3}, [AHA] = 6300 mol•m^{-3} recorded at pH = 0.44 at T = 313 K.

Figure 6: lnK_3 vs T^{-1} for the data of table 3, plotted in accordance with eq. 14 and describing the formation of the trisacetohydroxamatoiron (III) complex.

Figure 7: Speciation diagrams for Fe^{3+} - AHA system at 293 K showing concentrations of Fe^{3+}, FeL^{2+}, FeL_2^{+} and FeL_3 as functions of total AHA concentration (expressed as pHL) calculated at total ferric concentration of 2.5 mol•m^{-3} and $[HNO_3]$ = (a) 6000 mol•m^{-3}; (b) 1000 mol•m^{-3} and (c) 10 mol•m^{-3}

Figure 8: Speciation diagrams for Fe^{3+} - AHA system at 293 K showing concentrations of Fe^{3+}, FeL^{2+}, FeL_2^{+} and FeL_3 as functions of pH calculated at total ferric concentration of 2.5 mol•m^{-3} and total [AHA] = (a) 2.5 mol•m^{-3} and (b) 250 mol•m^{-3}, corresponding to AHA:Fe ratios of 1:1 and 100:1 respectively.

Figure 9: Speciation diagrams for Fe^{3+} - AHA system at pH = 1 showing concentrations of Fe^{3+}, FeL^{2+}, FeL_2^{+} and FeL_3 as functions of total AHA concentration (expressed as pHL) calculated at total ferric concentration of 25 mol•m^{-3} and T = (a) 293 K and (b) 323 K.

Figure 10: Speciation diagrams for Fe^{3+} - AHA system at [total AHA] = 250 mol•m^{-3} showing concentrations of Fe^{3+}, FeL^{2+}, FeL_2^{+} and FeL_3 as functions of pH calculated at total ferric concentration of 2.5 mol•m^{-3} and T = (a) 293 K and (b) 323 K.

Figure 11: Speciation diagrams for Fe^{3+} - AHA system, showing concentrations of Fe^{3+}, FeL^{2+}, FeL_2^{+} and FeL_3 as functions of pH calculated for concentrations of [Fe^{3+}] = 50 mol•m^{-3}, [AHA] = 1 mol•m^{-3} and T = (a) 293 K and (b) 323 K.

Figure 12: Speciation diagrams for Fe^{3+} - AHA system, showing concentrations of Fe^{3+}, FeL^{2+}, FeL_2^{+} and FeL_3 as functions of pH calculated for concentrations of [Fe^{3+}] = 0.5 mol•m^{-3}, [AHA] = 200 mol•m^{-3} and T = (a) 293 K and (b) 323 K.

Figure 13: Speciation diagrams for Fe^{3+} - AHA system, showing concentrations of Fe^{3+}, FeL^{2+}, FeL_2^{+} and FeL_3 as functions of pH calculated for concentrations of [Fe^{3+}] = 0.4 mol•m^{-3}, [AHA] = 6300 mol•m^{-3} and T = (a) 293 K and (b) 323 K.

Tables

T/K	Abs(510 nm) pH = 0.20	Abs(510 nm) pH = 0.71	Abs(510 nm) pH = 0.85	Average K_1 / unitless	Standard deviation
293	0.803	0.921	0.912	65.25	0.68
298	0.793	0.916	0.902	40.65	5.79
303	0.793	0.912	0.889	28.22	11.4
313	0.779	0.894	0.877	14.58	4.17
323	0.667	0.858	0.842	4.24	0.54

Table 1: Determination of K_1 in accordance with eq. 13 as a function of temperature, calculated from solutions with $[Fe^{3+}]_i = 50$ mol•m^{-3} and $[AHA]_i = 1$ mol•m^{-3}

T/K	Abs_{mono}-(510 nm)			Abs_{bis}-(470 nm)			Average K_2 / unitless	Standard deviation
	pH = 0.40	pH = 0.61	pH = 0.74	pH = 0.40	pH = 0.61	pH = 0.74		
293	0.419	0.199	0.080	0.338	0.505	0.696	2.638	2.055
298	0.449	0.190	0.085	0.317	0.512	0.691	2.561	1.934
303	0.449	0.199	0.090	0.314	0.502	0.686	2.340	1.782
313	0.469	0.239	0.120	0.285	0.464	0.656	1.759	1.175
323	0.489	0.259	0.140	0.241	0.431	0.629	1.438	0.9488

Table 2: Determination of K_2 in accordance with eq. 19 as a function of temperature calculated from solutions with $[Fe^{3+}]_i = 0.5$ mol•m^{-3} and $[AHA]_i = 200$ mol•m^{-3}

T/K	Abs_{bis}-(470 nm)			Abs_{tris}-(420 nm)			Average K_3 / unitless	standard dev^n
	pH = 0.44	pH = 0.84	pH = 0.93	pH = 0.44	pH = 0.84	pH = 0.93		
293	0.540	0.370	0.086	0.341	0.656	0.200	0.0151	0.0015
298	0.510	0.360	0.085	0.434	0.670	0.198	0.0179	0.0038
303	0.490	0.330	0.080	0.473	0.802	0.200	0.0222	0.0057
313	0.450	0.290	0.075	0.543	0.842	0.206	0.0274	0.0080
323	0.380	0.270	0.070	0.553	0.856	0.210	0.0323	0.0091

Table 3: Determination of K_3 in accordance with eq. 23 as a function of temperature calculated from solutions with $[Fe^{3+}]_i = 0.4$ mol•m^{-3} and $[AHA]_i = 6300$ mol•m^{-3}

	K@293K unitless	ΔH^o / kJ•mol^{-1}	ΔS^o / J•mol^{-1}•K^{-1}	ε / m^2•mol^{-1}
mono-	62.46	–56.4	–158.2	101
bis-	2.81	–17.09	–49.7	165
tris-	1.58×10^{-2}	+19.74	+32.93	363

Table 4: Thermodynamic data relating to the formation of the mono-, bis- and tris-AHA-Fe(III) complexes

Figures

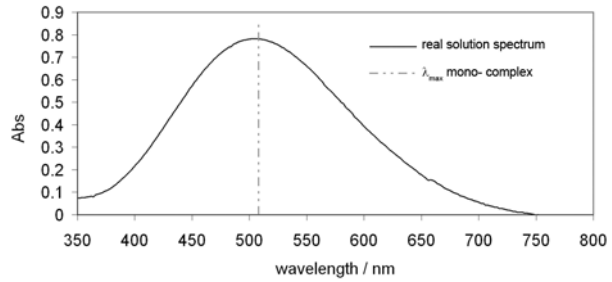

FIGURE 1

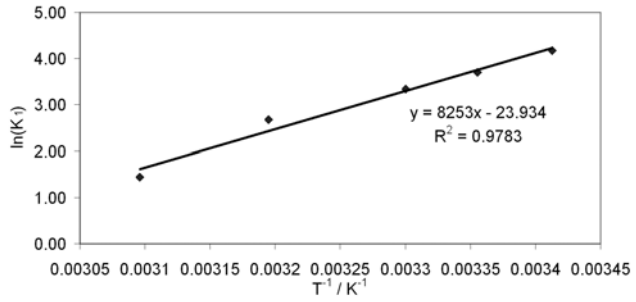

FIGURE 2

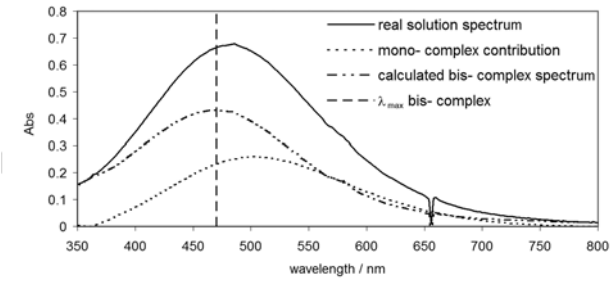

FIGURE 3

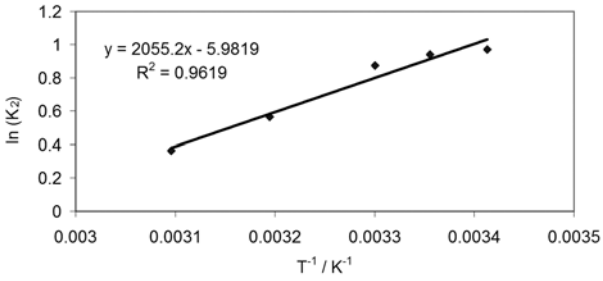

FIGURE 4

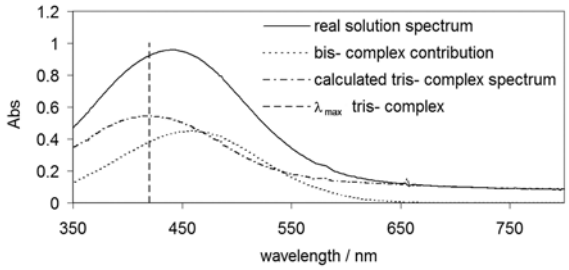

FIGURE 5

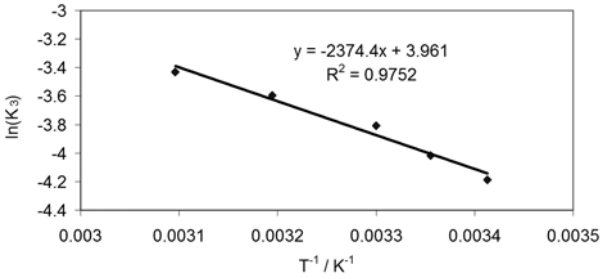

FIGURE 6

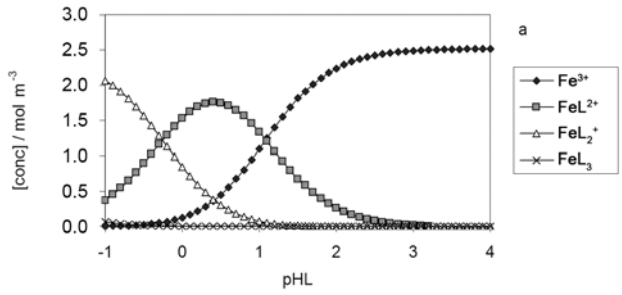

FIGURE 7A

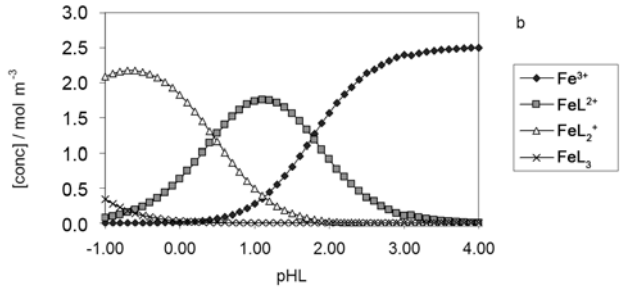

FIGURE 7B

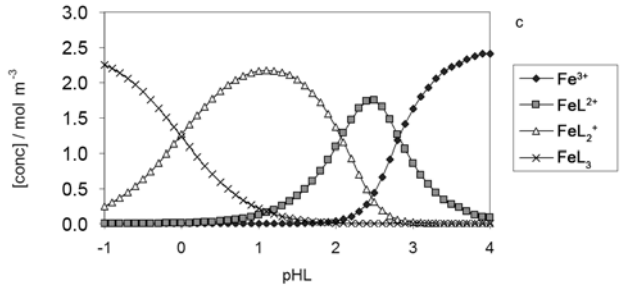

FIGURE 7C

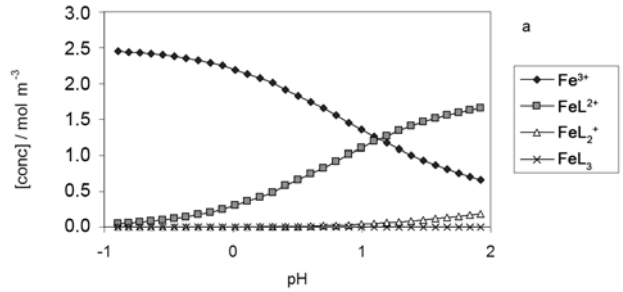

FIGURE 8A

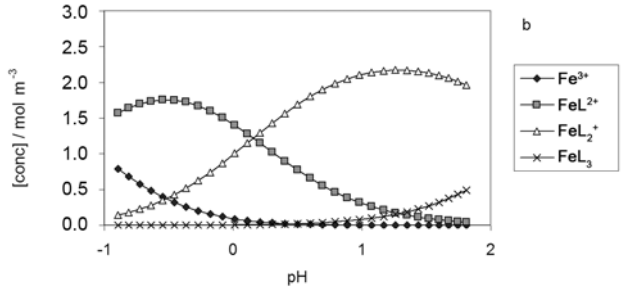

FIGURE 8B

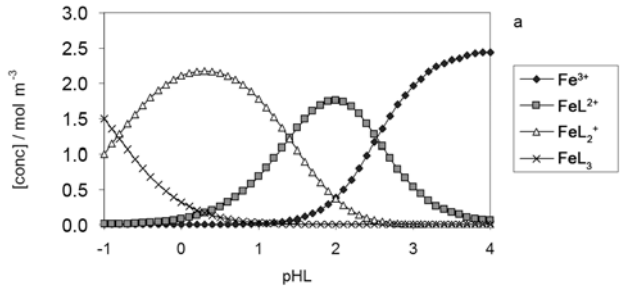

FIGURE 9A

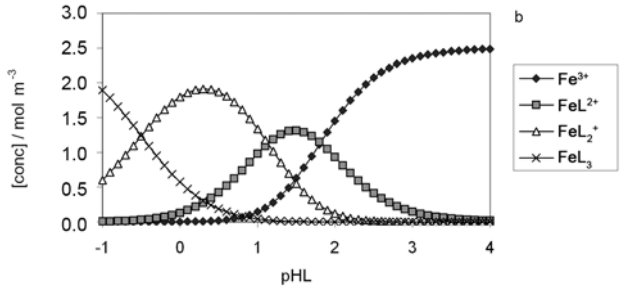

FIGURE 9B

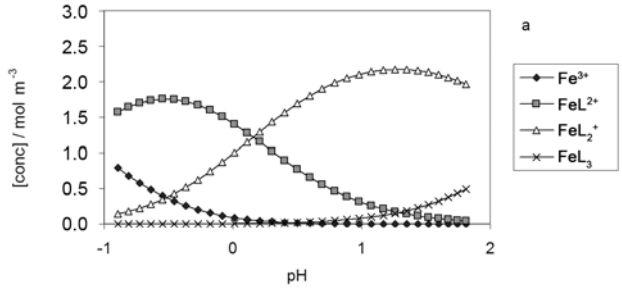

FIGURE 10A

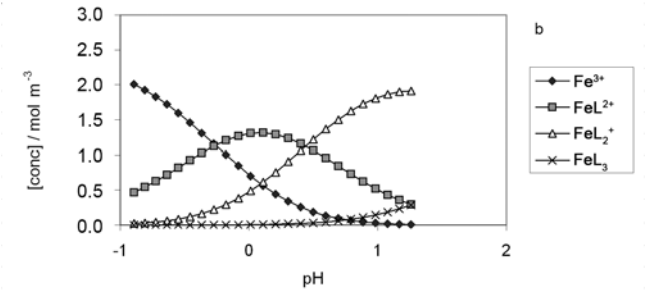

FIGURE 10B

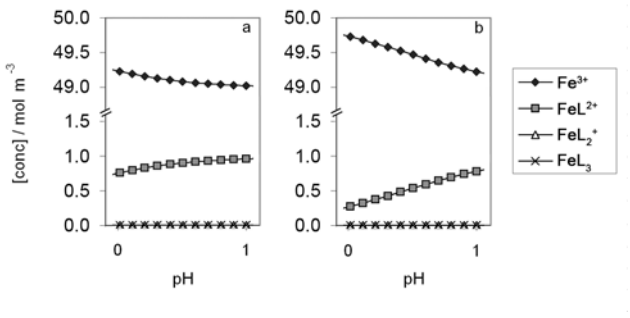

FIGURE 11

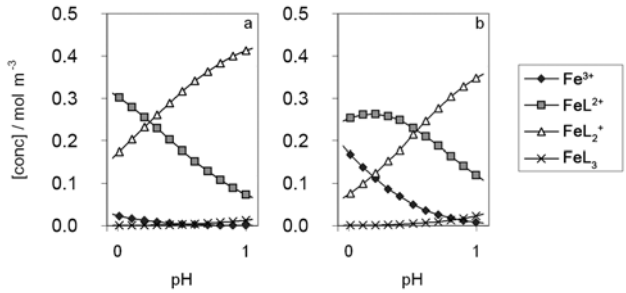

FIGURE 12

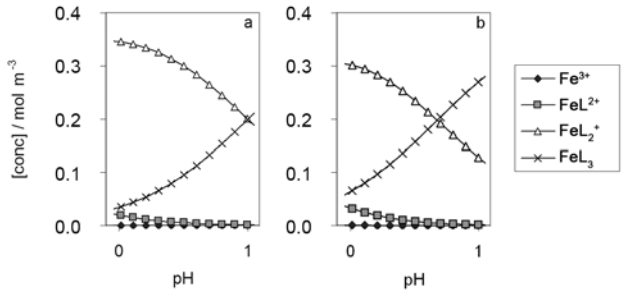

FIGURE 13